Digital Filtering Applications to the Lead Slowing-Down Spectrometer

Kathryn D. Huff

***Abstract*-This work investigates the method of application of Digital Filtering to the Lead Slowing-Down Spectrometer (LSDS). With a digital filter, a signal can be mathematically smoothed and reorganized, producing a more easily analyzable data set. Using two stages of differentiation to flatten background shapes and one of smoothing, we have been able to extend the useful range of measurements obtained from the LSDS at the Los Alamos Neutron Science Center (LANSCE).**

I. Introduction

The LSDS uses a pulsed neutron source and a compensated fission chamber to produce an output signal in the form of voltage vs. time. In such neutron-induced cross section measurements using a pulsed neutron source, data are often lost on complex backgrounds. This results in the need for a dead time correction particularly at high energies where saturation due to other processes creates a dramatically sloping background. Digital filtering can help to overcome this difficulty.

The goal of this project was to write a C++ code for use in data analysis to extend the range of analyzable LSDS data to 100 keV or more. This report describes the procedures used to filter the data and to derive a cross section from the waveforms.

II. Approach

First, the histograms of raw data were fit to determine the specific settings under which the measurements were taken (i.e. gain, interval, etc.). This information made it possible to create automated calibrations in the code.

Once this was accomplished, the next step became the application of the digital filter to LSDS data taken on a 70 µg sample of ^{235}U. This filter estimates the second derivative of the original waveform and also applies a modified triangular smoothing filter [1]:

$$\frac{d^2V_i}{dt^2} \approx \frac{g\,(V_{m+1+i} - V_{1+i} - V_{-1+i} + V_{-m-1+i})}{256\,\Delta_t^2\; m\,(m+2)}\,.$$

Here, g represents the full scale voltage of the eight bit digitizer, V is the sample value (Volts), m is a smoothing parameter, i loops through the whole waveform, and Δ_t is the sampling interval (for the run in this report, Δ_t = 2 ns). It is important to note that, for neutron energies less than 100 keV, the LSDS produces a neutron energy correlated with time, after the initial pulse,

$$\langle E_n \rangle = \frac{K}{(t+t_0)^2}\,.$$

with the relationship:
Here $\langle E_n \rangle$ is the mean neutron energy, t is the time after the initial pulse and the constants have the values K=161.1 keVµs^2 and t_0 = 0.36 µs.

IIA. The Threshold

This filter flattens the slowly sloping background curves that appear during the saturation at the beginning of each waveform. Once these curves are flattened, the waveform shows only double derivatives of the original peaks on a flat, though noisy, background. This lack of a complex background makes it possible to set a constant threshold line above the noise (Fig. 1).

The threshold cannot avoid catching some narrow digitization noise on the sides of the peaks without excessive smoothing. Since such smoothing could cause a significant loss in statistics and accuracy, it is necessary to make a width cut, filtering out peaks detected to have a width lower than the cut. To detect the width of each event, a width histogram was developed by recording the distance in time between the point at which the waveform crossed the threshold in the upward direction and the point at which it crossed again in the downward direction. The width cut makes it possible to lower the threshold such that it just touches the noise, so that it is sure to catch all the peaks.

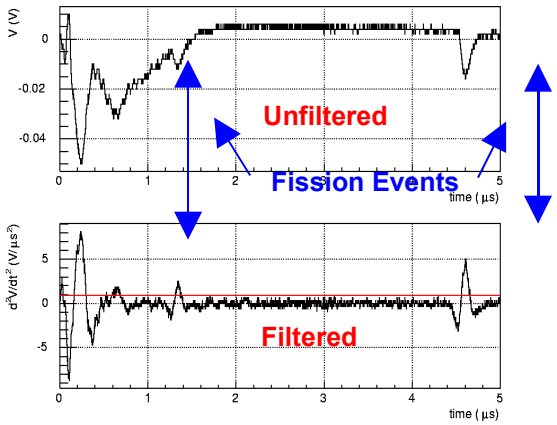

Fig. 1 The unfiltered waveform (top) has a background that is flattened by the smoothing double derivative filter so that a threshold (red) can be set on the filtered waveform (bottom) [1].

With this threshold, a histogram was filled each time a peak was identified with its time stamp and other derived data. A histogram of the neutron energy was divided by the neutron flux to deduce an un-normalized cross section.

The threshold for this step was determined using mostly qualitative analysis of the results in the width, energy, and time histograms. Distinct oscillations in the time and energy histograms indicated that the threshold was too low; whereas a sharp decrease in counts indicated that the inverse was true. In the width histogram, a ratio was taken of the very narrow peaks and the total peak count, and if that ratio was particularly high, the threshold was deemed to be too low. It became clear that the threshold was dependent on *m*, and by graphing the experimental estimates for threshold vs. *m*, it was determined that the threshold follows the digitization noise function:

$$\frac{6\,g}{m\,(m+2)\,t^2\,12^{1/2}\,2^{7.2}}\,.$$

The threshold values chosen subjectively correlate beautifully with this theoretical value (Fig. 2) except for the very low values of *m*, which result in a deviation from this estimation because of a lack of statistics. This means the noise is dominated by digitization noise. It is important to note that setting the digitizer to a higher sensitivity, value of *g*, would reduce the noise level due to digitization[1].

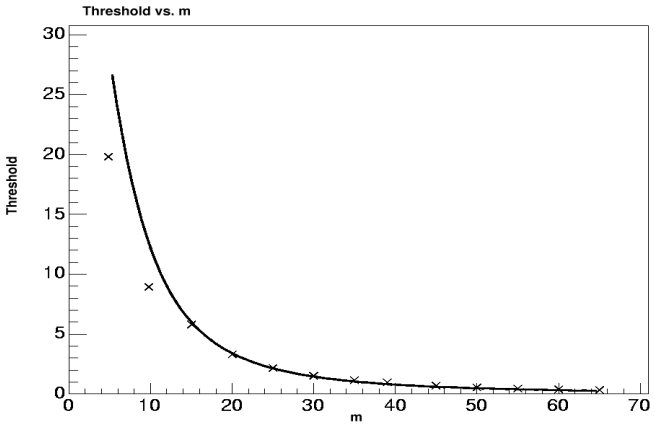

Fig. 2 Correlation between the experimental values chosen for the threshold and values of the smoothing parameter m. The points (x) determined by analysis are compared with the theoretical estimation(curve).

IIB. The Width Cut

Two distinct peaks appeared in the width histogram (Fig. 3), and indicated that perhaps there was a real possibility of separating out alpha decays from the neutron fissions in the data since counts with widths between 16 and 40 ns seemed to be an entity of their own.

It is clear that the multitude of very narrow peaks (under 16 ns) that appear in this width histogram are mostly digitization noise, and therefore, should be removed with a width cut at 16 ns. The results of this width cut (Fig. 4) were encouraging. It is made clear by the time-independent drop in counts that the noise from the edges of the peaks has been cut out. Also, it is important to note the resultant disappearance of a peculiarity in the uncut histogram at 60 keV, which extends our useful range to 100 keV.

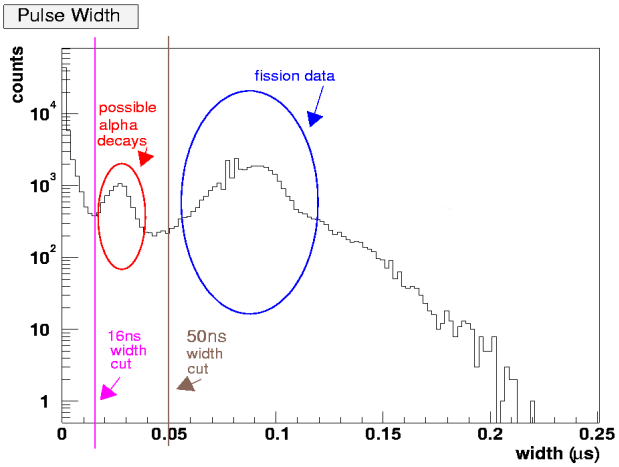

Fig. 3 The width cut at 16 ns (pink) would cut out only the very narrow peaks, while the width cut at 50 ns (brown) would cut out the counts seen in the first peak (red), while both cuts would leave the fission data (blue) uncut.

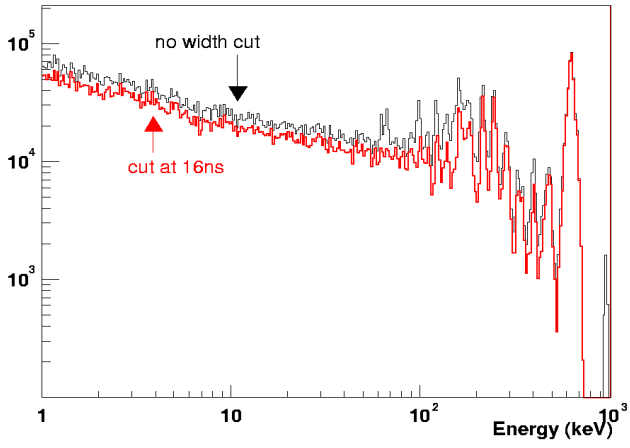

Fig. 4 Cross Section vs. Energy: The width cut at 16 ns (red) causes the disappearance of a peculiarity in the uncut histogram (black) at 60 keV.

If, in a width vs. time plot, the widths that formed the first peak in the width histogram were randomly dispersed through time, we might conclude that the small peak does represent alpha decay detection. However, the width vs. time plot (Fig. 5) did not show this random dispersal, and instead showed us that the widths in question occurred at the very beginning, in fact the first 0.1 μs, of each run indicating they resulted from saturation effects at short times, which is inconsistent with the behavior of alpha decay, which would appear in the histogram independent of time.

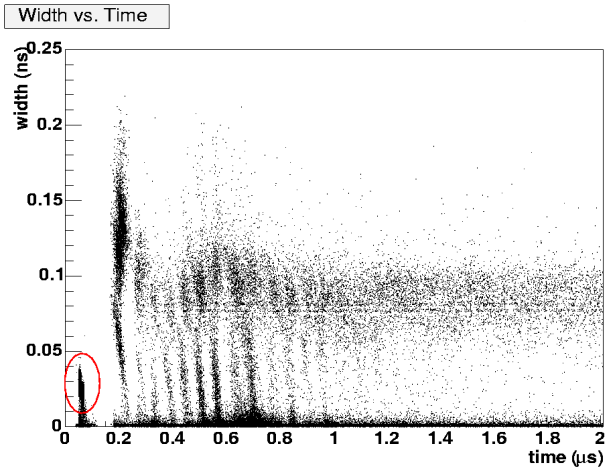

Fig. 5 This width vs. time plot shows that the width peak at 3 ns is dependent on time, indicating that they are not alphas, but instead an effect of the character of the early part of the waveforms.

Also, it should have been clear that no alpha decays could have been detected because of the very small sample size. With 70 μg of ^{235}U, a decay rate of 8.00E-02 per μg, analyzing 5500 waveforms, and with only 2 μs per waveform, for the entire set of waveforms we ran only approximately 0.0616 alpha decays could be expected, which would never have been visible.

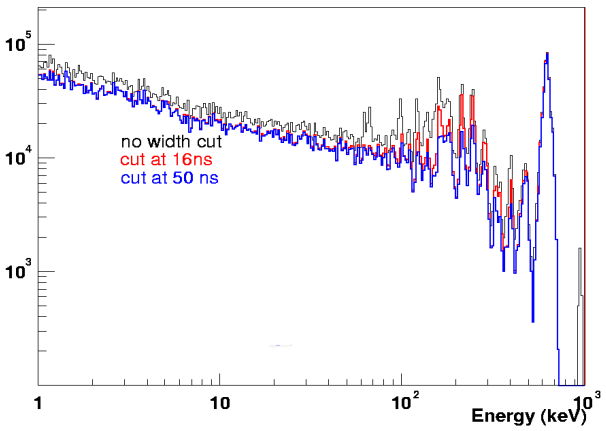

Fig. 6 The width cut at 50 ns (blue) results in a filtering of high energy noise even beyond that of the 16 ns cut (red).

Since the background occurrences that caused the smaller width peak (Fig. 3, red) are at such very high energies, they do not affect the range of data that we are interested in. However, a width cut at 50 ns might remove the tail of the narrowest width peak, thereby extending the useful range of the LSDS data. In fact, putting a width cut at 50 ns resulted in just that (Fig. 6).

IIc. Choosing *m*

The variable *m*, the smoothing parameter, is an important part of the digital filter that determines the smoothness of the filtered waveform. As *m* grows larger, the filtered waveform becomes smoother. Based on the Fourier transform calculations of the peak shape, we made an initial estimate of $m = 39$.

To find a range of *m*, histograms were made and analyzed of theoretical cross section ratios vs. experimental cross section ratios, cross section vs. energy, and two different forms of original peak height vs. filtered peak height.

The graph of σ at 5 keV divided by σ at 95 keV vs. *m* (Fig. 7) indicates that $m<25$ is inadequate because of a lack of samples in this low range, which can be seen in the resulting large error bars. This graph also indicates that, since the error bars do not change as *m* is increased beyond 39 and that the central value remains steady, there is no apparent upper limit to *m* where the cross section slope is concerned.

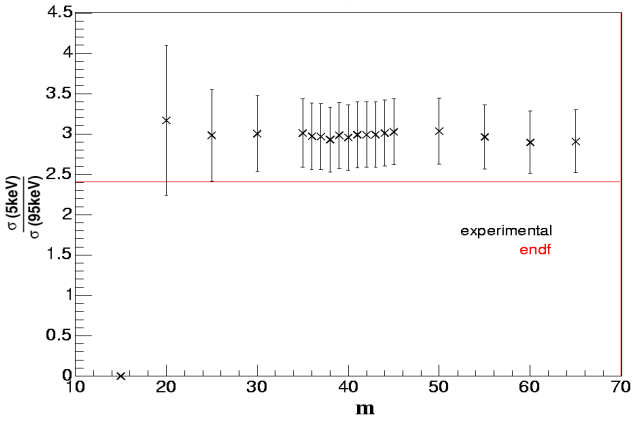

Fig. 7 The ratio of σ at 5keV and σ at 95keV vs. *m*: The accepted ENDF value for this ratio is shown in red [2].

For a few incremented *m* values, histograms were produced of the unfiltered peak area vs. the widths of the filtered peaks (Fig. 8,9). To create these graphs, the

program returns to the original histogram at each peak detected in the filtered waveform. The program then sums the unfiltered peak for 330 ns centered on the maximum peak location found in the second derivative. To remove the background, the program sums the same distance nearby in the waveform and subtracts that from the peak sum. In this fashion, it finds peaks with the filtered waveform, and integrates the corresponding peak in the original waveform. There is a distinct correlation between width and peak height for the filtered waveform, so the comparison of the integral of the peak to the width of the filtered peak is similar to a comparison of their relative peak heights.

The fission data are represented here (Fig 8,9) by the horizontal band just below zero. In the lower values of *m*, an area of the noise identified as a feature of the saturation, begins to overlap the real data, but because it is a feature of saturation, time will filter it out independent of width.

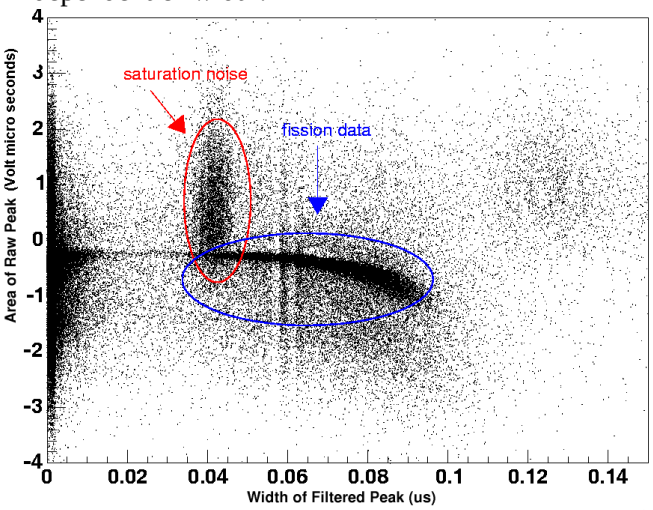

Fig. 8 Where *m* = 30, the red ellipse indicates the noisy area begins to move right, overlapping the fission data (blue) which is in turn moving left to merge with the noise.

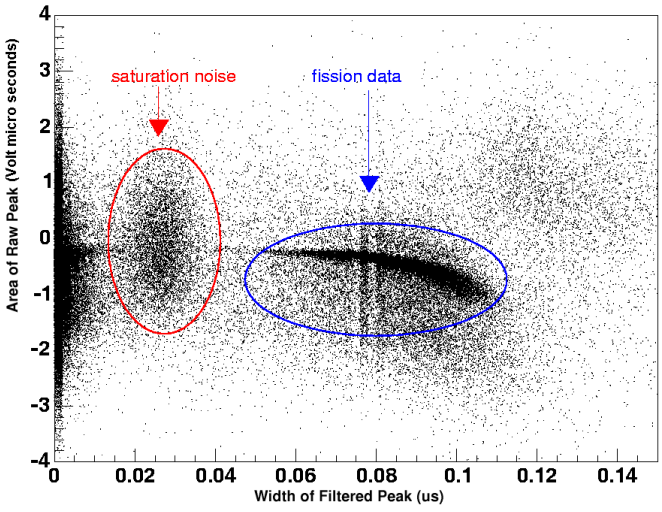

Fig. 9 Where *m* = 39, the red ellipse indicates the noisy area caused by a feature of the saturation. The fission data is in blue.

It may seem strange that these unfiltered peak area vs. filtered width graphs have positive readings. This is because there are some positive peaks in the original waveform due to saturation effects at short times and, to a lesser extent, due to unknown causes at longer times. The filtering and threshold algorithms used here do not eliminate these features [1].

The vertical banding that occurs in figures 8 and 9 is a result of a stair stepping effect in the digitization that creates horizontally flat spots on the downward side of small filtered peaks, which are more sensitive to its effects. These flat spots occur directly where the threshold intersects the waveform, such that the width is not read correctly, but, in fact, is read on either side of the stair step. The width can be measured on either side of its actual value, but not on it [1].

It is also important to note that the fission data begin to move into the noisier region to its right, a region resultant of positive peaks in the unfiltered waveform, as m increases. Therefore, since collision between the fission data and this noise region is undesirable, but since the number of these events is small, a very flexible upper limit of *m* at about 40 is reached.

The graph of cross section vs. energy for *m*=39 compared to *m*=45 (Fig. 10) provides more definition for the upper limit for *m* that was being sought. Because of visibly increasing noise levels and increasing deviations from the accepted cross section value, it becomes entirely clear that there is a soft upper limit at $m \approx 45$, which, though it is outside the range we have already established, adds definition to the previous vague upper limit of 40.

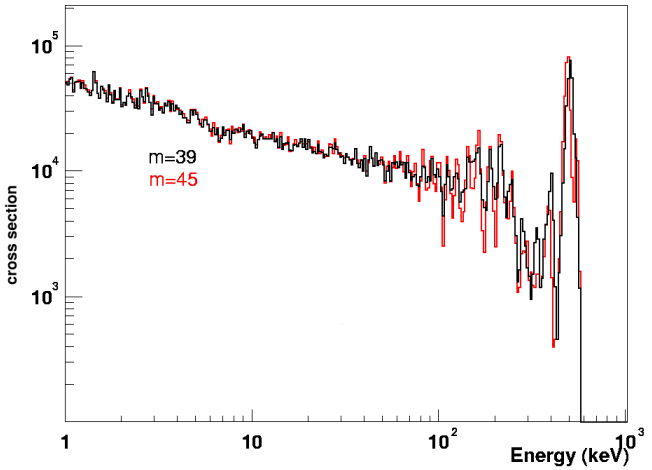

Fig. 10 cross section vs. Energy(keV) shows that *m* = 45, represented here in red, is too large and creates too much noise.

It seems clear, since *m* should be effective between 25 and 45, that 39 is an acceptable choice for *m*, but it is important to be certain that, once filtered, the LSDS measurement for the cross section matches the accepted cross section from the Nuclear Data Files [2]. A graph was therefore created of this (Fig. 11), and it seems that, with filtering, and even without a dead time correction, the data are useful up to at least 100 keV, thereby reaching the goal of the project and surpassing previous methods by a factor of five or more.

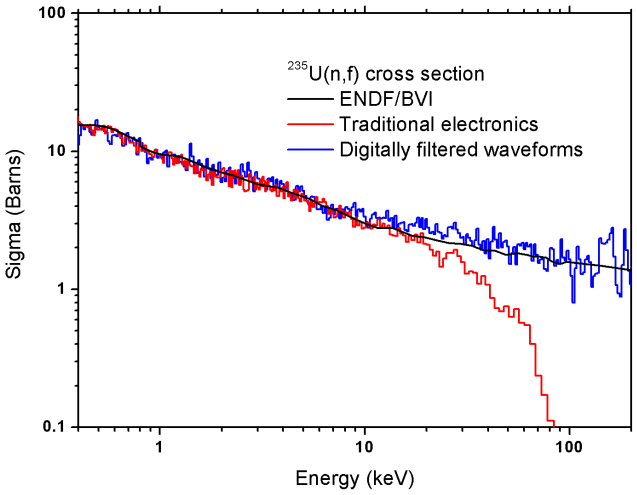

Fig. 11 The accepted ENDF neutron fission cross section for ^{235}U (black) agrees with the LSDS experimental results after digital filtering, even without a dead time correction (blue). The results of analysis of the same data with a previous method (red) begin to droop at about 20 keV without a dead time correction [2].

III. Conclusion

This report illustrates how the analyzable data range was increased from 20 keV to 100 keV without a dead time correction, by exhibiting how 50 ns width cut was arrived at and how it was determined that the ideal value of *m* for this particular application lies between 25-45. There are various possible uses for this filtering technique, such as application to other detectors that produce waveforms with similar characteristics.

IV. References

[1] J. M. O'Donnell, Private Communication.
[2] ENDF/B-VI-LIBRARY, National Nuclear Data Center, On-Line Access: WWW.NNDC.BNL.GOV, File ENDF, Brookhaven National Laboratory.